SUPPLEMENTAL DATA AND METHODS

Arginine vasopressin infusion is sufficient to model clinical features of preeclampsia in mice

Jeremy A. Sandgren[1], Guorui Deng[1], Danny W. Linggonegoro[1], Sabrina M. Scroggins[2], Katherine J. Perschbacher[1], Anand R. Nair[1], Taryn E. Nishimura[2], Shao Y. Zhang[1], Larry N. Agbor[1], Jing Wu[1], Henry L. Keen[1], Meghan C. Naber[1], Nicole A. Pearson[1], Kathy A. Zimmerman[3], Robert M. Weiss[3], Noelle C. Bowdler[2], Yuriy M. Usachev[1], Donna A. Santillan[2,6], Matthew J. Potthoff[1,6,7,8,9], Gary L. Pierce[4,6,7], Katherine N. Gibson-Corley[5,6,8], Curt D. Sigmund[1,6,7,8,9], Mark K. Santillan[2,6,*], and Justin L. Grobe[1,6,7,8,9,*]

[*] *co-corresponding authors*

[1]Department of Pharmacology, University of Iowa, Iowa City, IA 52242 USA
[2]Department of Obstetrics & Gynecology, University of Iowa, Iowa City, IA 52242 USA
[3]Department of Internal Medicine, University of Iowa, Iowa City, IA 52242 USA
[4]Department of Health & Human Physiology, University of Iowa, Iowa City, IA 52242 USA
[5]Department of Pathology, University of Iowa, Iowa City, IA 52242 USA
[6]University of Iowa Hospitals & Clinics Center for Hypertension Research, University of Iowa, Iowa City, IA 52242 USA
[7]François M. Abboud Cardiovascular Research Center, University of Iowa, Iowa City, IA 52242 USA
[8]Fraternal Order of Eagles' Diabetes Research Center, University of Iowa, Iowa City, IA 52242 USA
[9]Obesity Research & Education Initiative, University of Iowa, Iowa City, IA 52242 USA

Running head: AVP receptors and preeclampsia

Correspondence:
Justin L. Grobe, PhD, FAHA
Department of Pharmacology
51 Newton Rd., 2-307 BSB
Iowa City, IA 52242
Tel: (319) 353-5789
Email: justin-grobe@uiowa.edu

Co-corresponding author:
Mark K. Santillan MD, PhD, FACOG, FAHA
Department of Obstetrics and Gynecology
200 Hawkins Drive
Iowa City, IA 52242
Tel: (319) 356-3180
Email: mark-santillan@uiowa.edu

Supplemental Methods

Plasma osmolality and electrolytes
Trunk blood samples were collected after CO2 asphyxiation into tubes coated with EDTA (for plasma). Samples were then centrifuged (5,000 x g for 10 min) and the supernatant transferred to a separate tube and frozen at -80°C until analysis. Osmolality was measured using freezing-point depression (Fiske) and clinical chemistries determined using a handheld analyzer (iSTAT, Abbott Labs, Chem8+ cartridges).

Aspartate aminotransferase (AST) and alanine aminotransferase (ALT) activities
AST and ALT activity were determined in plasma samples using colorimetric assay kits (Sigma MAK055 and MAK052, respectively) according to the manufacturer's instructions.

Immunohistochemical detection of cytokeratin-8 (CK8)
CK8 immunostaining was performed on the same tissue sections examined with HE staining. Briefly, antigen unmasking of all paraffin sections was performed (citrate buffer, pH 6) in a decloaker. Endogenous peroxidase activity was quenched with 3% hydrogen peroxide, and 10% goat serum was used to block non-specific staining. Sections were incubated with rabbit monoclonal CK8/18 (Abcam Ab53280). Slides were then incubated with the appropriate secondary antibody and detection (DAKO Rabbit Envision HRP System reagent for 30 minutes). Slides were developed with DAKO DAB plus for 5 minutes followed by DAB Enhancer for 3 minutes before being counterstained with hematoxylin. Finally, CK8-stained slides were analyzed to measure the depth of CK8 immunoreactive cells into the decidua. To determine the maximum invasion depth of CK8 immunoreactive cells, two separate yet adjacent 5um thick tissue sections were measured from 4-7 fetoplacental units per dam, and 4-6 dams per group.

Supplemental Table 1: Diseases or cellular functions modified by AVP-infusion.

Diseases or Functions Modified by Gestational AVP-infusion	Molecules	p-value
Hypertension	C4orf33, HMGCR, LMF1, PDE10A, RORA, SCNN1G, SEMA5A, SLC39A8, TMEM135	5.07E-03
Abnormal morphology of cardiovascular system	DISP1, GATA2, LOXL2, NFAT5, PIM3, SEMA5A, TRPM2	1.68E-02
Abnormal morphology of heart	DISP1, GATA2, LOXL2, NFAT5, TRPM2	3.01E-02
Familial hypercholesterolemia	HMGCR, ITIH4	5.99E-03
Thrombosis of vein	HMGCR, PDE10A	2.39E-02
Transient ischemic attack	HMGCR, PDE10A	2.45E-03
Preeclampsia	**C4orf33, HMGCR, LMF1, SEMA5A, SLC39A8, TMEM135**	**1.01E-02**
Morphology of cardiovascular system	DISP1, GATA2, HMGCR, LOXL2, NFAT5, PIM3, RAPGEF3, SEMA5A, TRPC1, TRPM2	8.86E-03
Function of cardiomyocytes	ASPH, TRPM2	8.71E-03
Cell movement of endothelial cells	ARHGAP24, BCAS3, LOXL2, RAPGEF3, SEMA3F, SEMA5A	6.55E-03
Morphology of heart	DISP1, GATA2, HMGCR, LOXL2, NFAT5, RAPGEF3, TRPC1, TRPM2	1.27E-02
Morphology of heart ventricle	HMGCR, LOXL2, NFAT5, RAPGEF3, TRPM2	1.11E-02
Size of heart ventricle	RAPGEF3, TRPM2	1.19E-02
Angiogenesis	ARHGAP24, GATA2, LOXL2, NFAT5, PIM3, RAPGEF3, RORA, SEMA3F, SEMA5A, TCF4, TRPC1, UNC13B	2.69E-03
Development of endothelial tissue	ARHGAP24, LOXL2, SEMA3F, SEMA5A, UNC13B	2.68E-02
Cell cycle progression	DNA2, ESPL1, FYN, GATA2, MXI1, PIM3, PUM1, RAPGEF3, SEMA3F, TCF4, TRIM39, ZNF655	6.61E-03
Exit from cell cycle progression	GATA2, MXI1, RAPGEF3	3.21E-04
Cell death	AES, CERS2, ESPL1, FYN, GATA2, HMGCR, ILF3, ISG20, ITIH4, LOXL2, MBOAT7, MXI1, NFAT5, NFIB, PIM3, Prl3d1 (includes others), PUM1, RAPGEF3, SEMA3F, SPIN1, TBC1D24, TCF4, TESK2, TRIM39, TRPC1, TRPM2, UBQLN1, UNC13B, ZMYND11	2.86E-03

Apoptosis	AES, CERS2, ESPL1, FYN, HMGCR, ILF3, ITIH4, LOXL2, MBOAT7, MXI1, NFAT5, NFIB, PIM3, PUM1, RAPGEF3, SEMA3F, TCF4, TESK2, TRIM39, TRPC1, TRPM2, UBQLN1, UNC13B, ZMYND11	3.02E-03
Necrosis	CERS2, FYN, GATA2, ITIH4, MBOAT7, MXI1, NFAT5, NFIB, PIM3, Prl3d1 (includes others), RAPGEF3, SEMA3F, SPIN1, TBC1D24, TCF4, TESK2, TRIM39, TRPC1, TRPM2, UBQLN1, UNC13B, ZMYND11	1.62E-02
Cell death of embryonic cell lines	FYN, TCF4, TRIM39, TRPM2, ZMYND11	2.77E-02
Necrosis of epithelial tissue	CERS2, FYN, ITIH4, SEMA3F, TCF4, TRIM39, TRPM2, ZMYND11	8.26E-03
Cell death of epithelial cells	CERS2, FYN, ITIH4, TCF4, TRIM39, TRPM2, ZMYND11	1.01E-02
Cell death of epithelial cell lines	FYN, TCF4, TRIM39, TRPM2, ZMYND11	1.04E-02
Cell death of kidney cell lines	FYN, TCF4, TRIM39, TRPM2, UNC13B, ZMYND11	2.82E-03
Apoptosis of kidney cell lines	TCF4, TRIM39, UNC13B, ZMYND11	2.11E-02
Morphology of cells	ARHGAP24, CERS2, DNA2, ESPL1, FYN, GATA2, ILF3, LOXL2, MBOAT7, MXI1, NFIB, PIM3, Prl3d1 (includes others), RAPGEF3, RORA, SEMA3F, SEMA5A, STYX, TCF4, TRPC1, TRPM2, UNC13B	1.32E-03
Abnormal morphology of cells	DNA2, ESPL1, FYN, ILF3, MBOAT7, MXI1, NFIB, PIM3, RAPGEF3, SEMA5A, STYX, TRPM2, UNC13B	1.66E-02
Sprouting	FYN, PIM3, SEMA3F, SEMA5A, TBC1D24, TRPC1, UNC13B	3.36E-03
Branching of cells	FYN, LOXL2, PIM3, SEMA3F, TBC1D24, TRPC1	1.06E-02
Release of Ca2+	ASPH, FYN, IBTK, TRPM2	1.18E-02
Phagocytosis by macrophages	FYN, RAPGEF3, RORA	1.53E-02
Depolymerization of actin filaments	PLEKHH2, SEMA5A	3.19E-03
Differentiation of nervous system	DISP1, EBF3, GATA2, MBOAT7, NFIB, RAPGEF3, TCF4	1.07E-02
Proliferation of embryonic stem cell lines	GATA2, PIM3	2.94E-03
Development of B lymphocytes	FYN, RORA, TCF4	2.17E-02

Development of pro-B lymphocytes	FYN, TCF4	3.74E-03
Development of hematopoietic progenitor cells	FYN, GATA2, RORA, TCF4	2.65E-02
Development of neurons	EBF3, FYN, NCMAP, NFIB, RAPGEF3, SEMA3F, TBC1D24, TRPC1, UNC13B	2.00E-02
Ion homeostasis of cells	FYN, GATA2, IBTK, SCNN1G, SLC39A8, TRPC1, TRPM2	2.29E-02
Production of cells	FYN, PUM1, STYX	2.24E-02
Production of sperm	PUM1, STYX	9.26E-04
Flux of ion	FYN, IBTK, SCNN1G, SLC39A8, TRPC1, TRPM2	3.98E-03
Flux of inorganic cation	IBTK, SCNN1G, SLC39A8, TRPC1, TRPM2	1.34E-02
Cell movement	ARHGAP24, ASPH, BCAS3, EBF3, FYN, GATA2, ILF3, LOXL2, MBOAT7, NFAT5, RAPGEF3, SCNN1G, SEMA3F, SEMA5A, STYX, TBC1D24, TCF4, TMEM201, TRPC1, TRPM2, UNC13B	3.67E-03
Migration of cells	ARHGAP24, ASPH, BCAS3, EBF3, FYN, GATA2, ILF3, LOXL2, MBOAT7, NFAT5, RAPGEF3, SCNN1G, SEMA3F, SEMA5A, STYX, TBC1D24, TCF4, TMEM201, TRPC1, TRPM2	1.95E-03
Invasion of cells	ARHGAP24, ASPH, FYN, ILF3, LOXL2, NFAT5, RORA, SEMA3F, SEMA5A, TCF4, TRPC1	6.38E-03
Cell movement of neurons	EBF3, FYN, GATA2, MBOAT7, SEMA3F, TBC1D24, TRPC1	1.32E-04
Cell movement of cerebral cortex cells	SEMA3F, TBC1D24	1.66E-02
Guidance of axons	FYN, SEMA3F, SEMA5A	2.52E-02
Cell movement of gonadal cell lines	ARHGAP24, FYN	3.08E-02
Lipodystrophy	HMGCR, POLG	7.88E-03
Growth Failure	AES, ESPL1, NFAT5, PIM3, POLG, TCF4, TET1	2.87E-02
Familial mental retardation	EBF3, MBOAT7, TBC1D24, TTI2, ZMYND11	9.74E-03
Autosomal recessive mental retardation	MBOAT7, TBC1D24, TTI2	8.71E-03
Autosomal dominant mental retardation	EBF3, ZMYND11	2.86E-02
Polycystic Kidney Disease	GANAB, HEPH, HMGCR, RAPGEF3	2.32E-02
Autosomal dominant polycystic kidney disease	GANAB, HEPH, HMGCR	5.88E-03

Mental retardation	EBF3, MBOAT7, RORA, TBC1D24, TCF4, TTI2, ZMYND11	1.18E-03
Severe mental retardation	RORA, TCF4	7.85E-04
Congenital malformation of brain	DISP1, DNA2, MBOAT7, NFIB, UNC13B	1.83E-02
Replication of mitochondrial DNA	DNA2, POLG	1.08E-03
Formation of brain	EBF3, FYN, MBOAT7, NFIB, RAPGEF3, RORA, SEMA3F, SEMA5A, TCF4	9.04E-04
Formation of forebrain	EBF3, FYN, NFIB, SEMA5A	2.22E-02
Formation of hippocampus	FYN, NFIB, SEMA3F	9.94E-03
Development of body axis	AES, ASPH, DISP1, EBF3, FYN, GATA2, MBOAT7, NFIB, RAPGEF3, RORA, SEMA3F, SEMA5A, TCF4	2.98E-03
Development of head	AES, ASPH, EBF3, FYN, GATA2, MBOAT7, NFIB, RAPGEF3, RORA, SEMA3F, SEMA5A, TCF4	4.70E-03
Morphogenesis of head	ASPH, FYN, GATA2, NFIB	2.54E-02
Synthesis of reactive oxygen species	FYN, HEPH, ITIH4, POLG, RAPGEF3, RORA, TRPM2, UBQLN1	1.96E-03
Production of reactive oxygen species	FYN, HEPH, POLG, RAPGEF3, RORA, TRPM2, UBQLN1	1.41E-03
Expression of RNA	AES, BCAS3, EBF3, EIF3K, FYN, GATA2, IBTK, ILF3, ISG20, LOXL2, MXI1, NFAT5, NFIB, PC, RAPGEF3, RORA, SPIN1, TCF4, TET1, TMEM135, ZMYND11	2.92E-03
Transcription	AES, BCAS3, EBF3, FYN, GATA2, IBTK, ILF3, LOXL2, MXI1, NFAT5, NFIB, PC, RAPGEF3, RORA, SPIN1, TCF4, TET1, TMEM135, ZMYND11	6.89E-03
Transcription of RNA	AES, BCAS3, EBF3, GATA2, IBTK, ILF3, LOXL2, MXI1, NFAT5, NFIB, RAPGEF3, RORA, SPIN1, TCF4, TET1, ZMYND11	2.15E-02
Transcription of DNA	AES, BCAS3, EBF3, GATA2, ILF3, LOXL2, MXI1, NFAT5, NFIB, RAPGEF3, RORA, SPIN1, TCF4, TET1	2.10E-02
Hereditary bleeding disorder	GATA2, POLG	2.19E-02
Hyperlipoproteinemia	HMGCR, ITIH4, LMF1	7.21E-03
Dyslipidemia	HMGCR, LMF1, RORA	1.88E-02
Quantity of pre-B lymphocytes	FYN, PIM3, TCF4	1.20E-02
Quantity of steroid	HMGCR, PDE10A, POLG, Prl3d1 (includes others), RAPGEF3, RORA	2.43E-02
Disorder of lipid metabolism	HMGCR, LMF1, POLG, RORA	1.86E-02

Transport of ion	FYN, HEPH, SCNN1G, SEC14L1, SLC39A8, TRPC1, TRPM2	5.91E-03
Transport of cation	HEPH, SCNN1G, SEC14L1, SLC39A8, TRPC1, TRPM2	7.01E-03
Transport of metal ion	HEPH, SCNN1G, SLC39A8, TRPC1, TRPM2	1.20E-02
Secretion of protein	LMF1, RAPGEF3, UNC13B	3.05E-02
Development of central nervous system	EBF3, FYN, MBOAT7, NCMAP, NFIB, RAPGEF3, RORA, SEMA3F, SEMA5A, TCF4	1.41E-03
Myelination of central nervous system	FYN, NCMAP	7.88E-03
Abnormal morphology of brain	DISP1, FYN, MBOAT7, NFIB, RORA, SEMA3F	1.87E-02
Abnormal morphology of forebrain	DISP1, MBOAT7, NFIB, SEMA3F	1.43E-02
Abnormal morphology of hippocampus	FYN, MBOAT7, NFIB	9.52E-03
Abnormal morphology of dentate gyrus	FYN, NFIB	1.24E-02
Function of brain	FYN, RORA	2.93E-02
Morphology of forebrain	DISP1, FYN, MBOAT7, NFIB, SEMA3F	4.39E-03
Morphology of telencephalon	FYN, MBOAT7, NFIB, SEMA3F	8.51E-03
Movement Disorders	EBF3, EIF3K, HEPH, HMGCR, ILF3, ITIH4, PDE10A, POLG, RORA, SEMA5A, TBC1D24, TMEM200C, TMEM55A	3.36E-03
Cognitive impairment	EBF3, HMGCR, MBOAT7, RORA, TBC1D24, TCF4, TRPM2, TTI2, ZMYND11	3.58E-04
Seizure disorder	FYN, PIM3, POLG, RAPGEF3, SEMA3F, TBC1D24, UNC13B	9.76E-03
Seizures	PIM3, POLG, RAPGEF3, SEMA3F, TBC1D24, UNC13B	1.30E-02
Major depression	HMGCR, IBTK, ITIH4, PDE10A, SEMA3F	3.20E-03
Metabolism of cyclic GMP	PDE10A, RORA	1.41E-03
Abnormal morphology of renal tubule	FYN, MXI1, NFAT5	8.32E-03
Abnormal morphology of small kidney	FYN, MXI1	2.39E-02
Atrophy of kidney	MXI1, NFAT5	1.19E-02
Size of body	Celf1, FYN, ILF3, MBOAT7, PDE10A, PIM3, PUM1, RAPGEF3, SEMA3F, TET1, TRPC1	3.40E-03
Production of urine	POLG, SCNN1G	1.24E-03
Morbidity or mortality	AES, ASPH, DISP1, DNA2, ESPL1, FYN, GATA2, HMGCR, ILF3, MBOAT7, MXI1, NFAT5, NFIB, POLG, RORA, SCNN1G, SEMA5A, TCF4, TRPC1, TRPM2, UNC13B	1.25E-02

Organismal death	AES, ASPH, DISP1, DNA2, ESPL1, FYN, GATA2, HMGCR, ILF3, MBOAT7, MXI1, NFAT5, NFIB, POLG, RORA, SCNN1G, SEMA5A, TCF4, TRPC1, UNC13B	2.16E-02
Phosphorylation of protein	FYN, IBTK, ILF3, PELI2, PIM3, PRR5L, RAPGEF3, TESK2	1.73E-02
Major affective disorder	FYN, HMGCR, IBTK, ITIH4, PDE10A, SEMA3F	7.79E-03
Growth of epithelial tissue	ARHGAP24, CERS2, FYN, GATA2, ITIH4, LOXL2, NFIB, SEMA3F, SEMA5A, TCF4	1.94E-03

Supplemental Table 2: Upstream regulators with similar effects on RNA profile

Upstream Regulators	p-value
(5-(4-N-methyl-N(2-pyridyl)amino)ethoxy)benzyl thiazolidine-2,4-dione	0.035
2,2'-dipyridyl	0.018
ACAT1	0.011
apomine	0.011
ARHGAP21	0.010
ARHGDIA	0.045
ASIP	0.001
ATF6	0.019
ATP1A1	0.007
AVP	**0.012**
bavachalcone	0.007
Bcl9-Cbp/p300-Ctnnb1-Lef/Tcf	0.031
beta-cyclodextrin	0.038
biotin	0.042
BRD2	0.014
Ca^{2+}	**0.014**
carnosine	0.031
CASQ2	0.025
CERS3	0.007
CERS4	0.011
CERS5	0.011
chitosan	0.011
clofibrate	0.048
copper	0.045
CSK	0.038
CTNNB1	0.042
CYP51A1	0.045
DAB2	0.025
DAZ2	0.035
DBI	0.042
DDX17	0.038
desmopressin	**0.004**
DETA-NONOate	0.014
DHCR7	0.011
DNAJA2	0.011
DNAJB1	0.007
DOCK8	0.025
EHF	0.039
ERBB2	0.050
ESR1	0.002
FABP2	0.045
FABP5	0.002
Fe2+	0.038

Fe3+	0.004
FRK	0.018
GCLC	0.014
GDF2	0.040
geranylgeraniol	0.025
GPR17	0.011
HES5	0.035
HESX1	0.025
hormone	0.042
ibandronic acid	0.035
ID2	0.003
ID3	0.026
ILF2	0.007
iodoacetic acid	0.021
KMUP-1	0.038
LDLRAP1	0.011
lenalidomide	0.026
LSP1	0.018
MAD1L1	0.014
maneb	0.021
manidipine	0.025
MBTPS1	0.045
methapyrilene	0.002
mir-185	0.028
miR-29b-3p (and other miRNAs w/seed AGCACCA)	0.022
MLLT3	0.025
monensin	0.042
mono-(2-ethylhexyl)phthalate	0.021
nitrendipine	0.014
NKX2-1	0.026
NPC1L1	0.031
NUPR1	0.002
PAG1	0.011
PELP1	0.014
PEX5L	0.045
PHLDA2	0.018
pioglitazone	0.020
PLG	0.002
POMC	0.044
PP2A	0.042
PPARG	0.024
PRDM8	0.042
procaine	0.007
progesterone	0.005
pyridaben	0.016
RBBP7	0.042

RIMS1	0.007
risedronic acid	0.021
RNF139	0.007
RNF17	0.021
RNH1	0.011
RORA	0.031
SAMSN1	0.041
SASH1	0.026
SCNN1A	0.007
SCNN1B	0.018
SDCBP	0.048
SERPINA3	0.025
SLC12A2	0.021
SOAT1	0.028
SOCS2	0.048
SPHK2	0.048
SRT2183	0.014
ST8SIA1	0.038
STAT4	0.045
terbutaline	0.038
TGFB1	0.044
TPT1	0.048
TRDN	0.007
TRIM33	0.018
TRPC3	0.018
VEZF1	0.011
ZFHX3	0.041
ziprasidone	0.028

Supplemental Table 3: Blood chemistries on GD 17.5 from dams infused with saline or AVP.

	Na (mmol/L)	K (mmol/L)	Cl (mmol/L)	iCa (mmol/L)	Glucose (mg/dL)	BUN (mg/dL)	Creatinine (mg/dL)	Hematocrit (%)
Saline (n=11)	145.9 ± 0.6	7.5 ± 0.3	106.8 ± 0.9	1.25 ± 0.01	170.8 ± 6.1	19.8 ± 1.1	1.0 ± 0.1	35.7 ± 1.9
AVP (n=5)	143.4 ± 2.2	8.0 ± 0.5	103.8 ± 1.0	1.31 ± 0.09	173.8 ± 3.8	22.8 ± 0.8	1.0 ± 0.0	32.6 ± 5.5
p-value	0.16	0.32	0.06	0.31	0.76	0.12	0.98	0.50

Supplemental Table 4: GRD Hypoxia Gene List.

Genes					
ADM	CSRP2	GLRX	MAFF	PPFIA4	SRD5A3
ADORA2B	CXCR4	GPR87	MET	PRKCA	SRPX
AHNAK2	CYB5A	GYS1	MXI1	PTRF	STBD1
AK4	DAAM1	HEY1	NDRG1	QSOX1	STC1
AKAP12	DDIT4	HK2	NFIL3	RASA4	STC2
ALDOC	DPYSL2	HLA-DRB1	NOL3	RBCK1	TGFBI
ANG	DPYSL4	IGFBP3	NR3C1	RBPJ	TMEFF1
ANGPTL4	DSC2	IGFBP5	OBSL1	RLF	TMEM45A
ANKZF1	DST	ILVBL	OLFML2A	RNASE4	TNFAIP8
ARTN	DTNA	INHA	OPN3	RRAGD	TXNIP
ASPH	EFNA3	INSIG2	P4HA1	S100A2	UPK1A
ATF3	EGFR	ISG20	P4HA2	S100A4	VEGFA
ATG14	EGLN1	ITPR1	PAM	S100A6	VEGFC
ATXN1	EGLN3	JUN	PDGFB	SAMD4A	VLDLR
BHLHE40	EGR1	KDM3A	PDK1	SAT1	WISP2
BNIP3	ELF3	KDM4B	PFKFB3	SCNN1B	WSB1
BNIP3L	ENO2	KIAA1199	PFKP	SERPINE1	YEATS2
C7orf68	ERO1L	KLF6	PGAP1	SFXN3	YPEL1
CA9	FAM13A	KLF7	PGK1	SH3GL3	ZNF292
CADM1	FAM162A	KLHL24	PGM1	SLC2A1	ZNF395
CAV1	FOS	KRT15	PHLDA1	SLCO4A1	ZNF654
CCNG2	FYN	LIMCH1	PIM1	SOX9	
CD59	GBE1	LOX	PLAC8	SPAG4	
CITED2	GDF15	LOXL1	PLAUR	SPOCK1	
CSGALNACT1	GJA1	LOXL2	PLIN2	SPRY1	

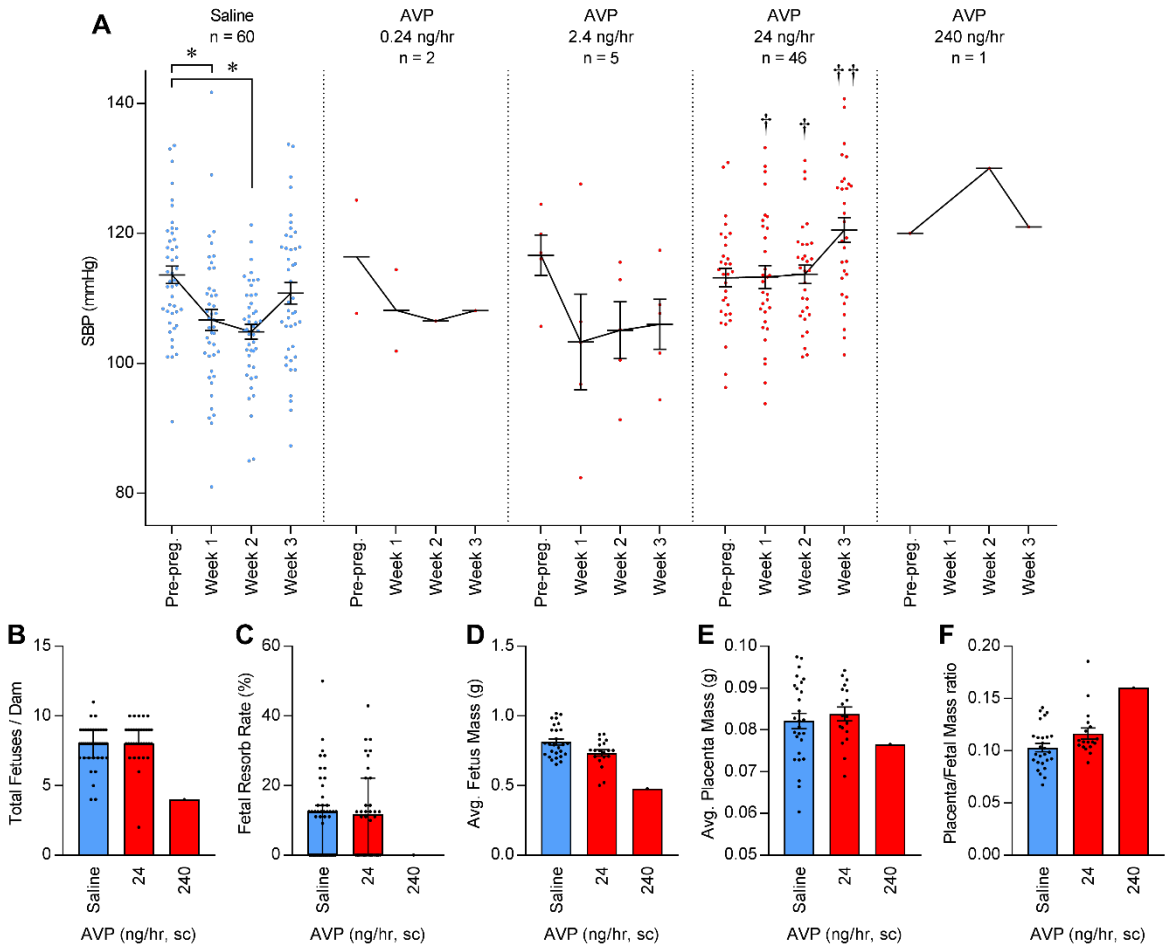

Supplemental Figure 1: *Preliminary dose-response studies support use of 24 ng/hr subcutaneous infusion of AVP, as lower doses (0.24 or 2.4 ng/hr) failed to elicit robust phenotypes while a higher dose (240 ng/hr) largely prevented pregnancy and caused severe growth restriction.* (**A**) Chronic infusion of saline resulted in expected mid-gestational reduction in systolic blood pressure (SBP). Chronic infusion of low (0.24 or 2.4 ng/hr) doses of AVP had no qualitative effect upon this pattern, however, chronic 24 ng/hr subcutaneous infusion of AVP qualitatively and quantitatively altered this pattern. AVP main effect p=0.01, gestational time p<0.01, and AVP x gestational time interaction p<0.0001. Notably, despite many attempts to generate pregnant mice with a 240 ng/hr infusion pump, only one mouse was successfully made pregnant and carried to term; this dam exhibited SBP values similar to the dams infused at 24 ng/hr. Analyses for saline, 2.4 and 24 ng/hr datasets performed by two-way ANOVA followed by Tukey's multiple-comparison procedure, with n's as indicated in figure (0.24 and 240 ng/hr datasets only shown for illustrative purposes, and not included in analytical comparisons). *p<0.05 as indicated. † p<0.05 vs saline at same gestational time-point. †† p<0.05 vs 2.4 ng/hr at same gestational time-point. (**B**) Total number of fetuses, (**C**) spontaneous fetal resorption rate, (**D**) average fetus mass, (**E**) average placental mass, and (**F**) average placental/fetal mass ratio (each per pregnant dam). Data shown in (A, D-F) as mean ± SEM, and in (B-C) as median ± interquartile range.

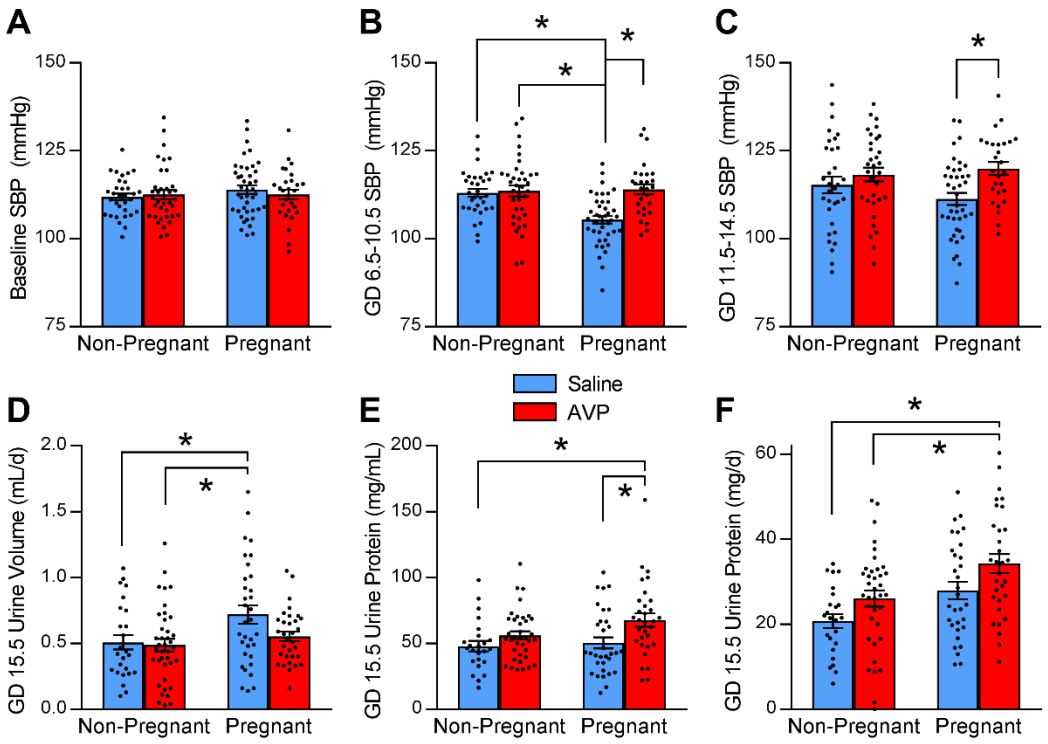

Supplemental Figure 2: *Pregnancy sensitizes the cardiovascular system to the effects of AVP.* Systolic blood pressure (SBP) determined before pump implantation (**A**), during mid-gestation at GD 6.5-10.5 (**B**), or late-gestation at GD 11.5-14.5 (**C**) compared with non-pregnant mice infused with AVP on the same timelines. *Mid-gestation*: Preg p<0.05, AVP p<0.05, PxA p<0.05. *Late-gestation*: Preg p=NS, AVP p<0.05, PxA p=NS. (**D**) Total 24-hour urine volumes collected on GD 15.5. Preg p<0.05, AVP p=NS, PxA p=NS. (**E**) Urine protein concentration on GD 15.5. Preg p=NS, AVP p<0.05, PxA p=NS. (**F**) Total protein lost to urine per day, calculated as the product of urine volume per day x urine protein concentration. Preg p<0.05, AVP p<0.05, PxA p=NS. In all panels, pregnant saline- and AVP-infused groups are replicated from Fig 6 in main text for clarity. (Non-preg+sal n=24-32, Non-preg+AVP n=37-40, Preg+sal n=42, Preg+AVP n=28). Analyses by 2-way ANOVA followed by Tukey procedure. Data shown as mean ± SEM. *p<0.05.

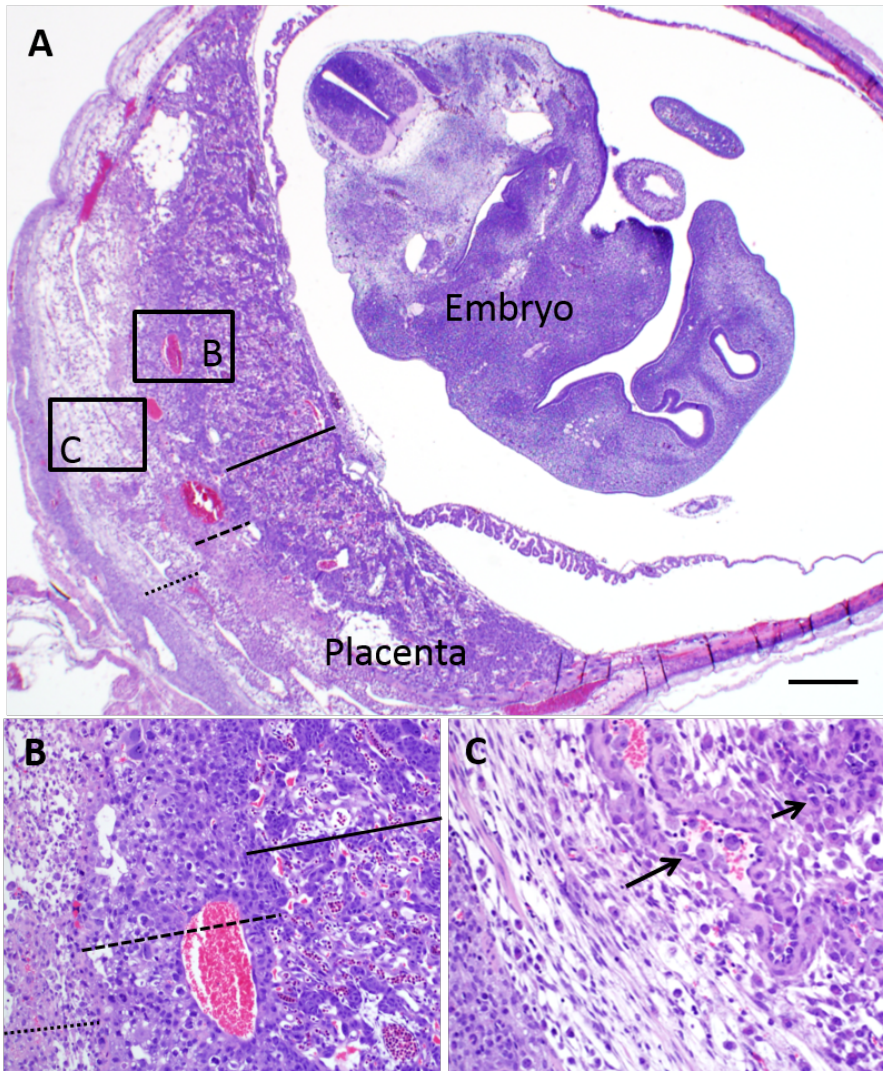

Supplemental Figure 3: *Methods of sectioning and measuring feto-placental units with hematoxylin & eosin stain.* (**A**) Murine fetoplacental unit sectioned at 5μm thickness and stained with hematoxylin & eosin, which contain both the embryo and placenta. Key placental layers indicated include the labyrinth layer (solid line), the spongiotrophoblast layer (wide dotted line) and decidua (narrow dotted line). Scale bar = 500 μm. (**B**) Higher magnification showing the morphology of the different placental layers. (**C**) Higher magnification of the decidua containing scattered spiral arteries that are surrounded by and sometimes contain plump round to polygonal trophoblast cells.

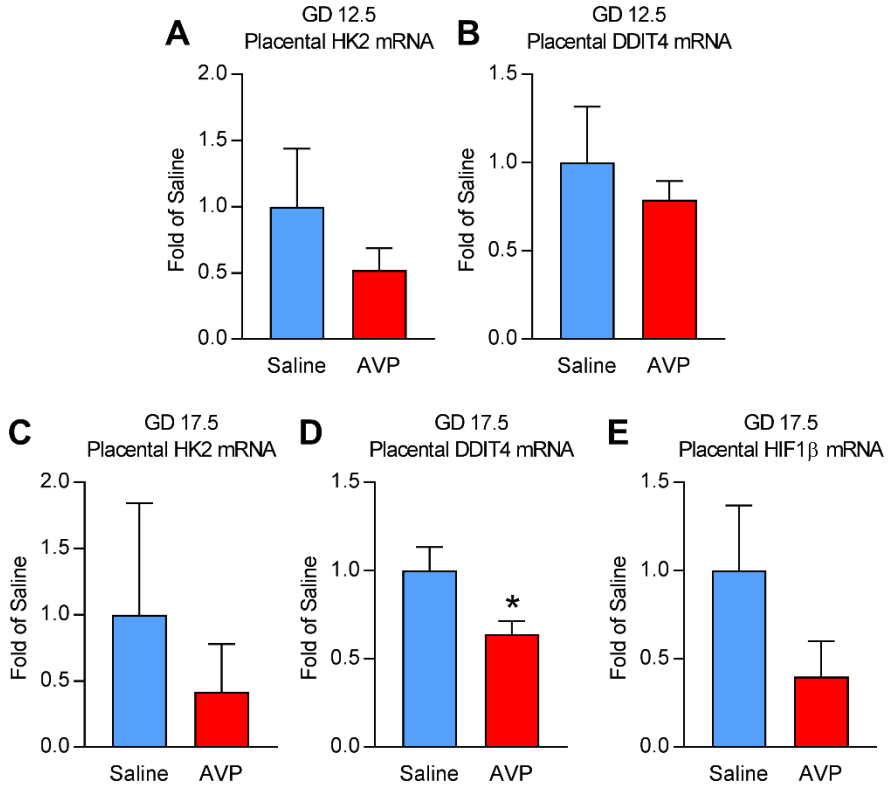

Supplemental Figure 4: *Hypoxia-inducible factor 1α (HIF1A) targets were not elevated with AVP-infusion.* Molecular markers of hypoxia in the placenta, (**A**) *Hk2* and (**B**) *Ddit4* at GD12.5 (Saline n=5, AVP n=8) and (**C**) *Hk2*, (**D**) *Ddit4*, and (**E**) *Hif1b* at GD 17.5 (Saline n=18, AVP n=21). Analyses by Student's T-test. Data shown as mean ± SEM. *p<0.05.

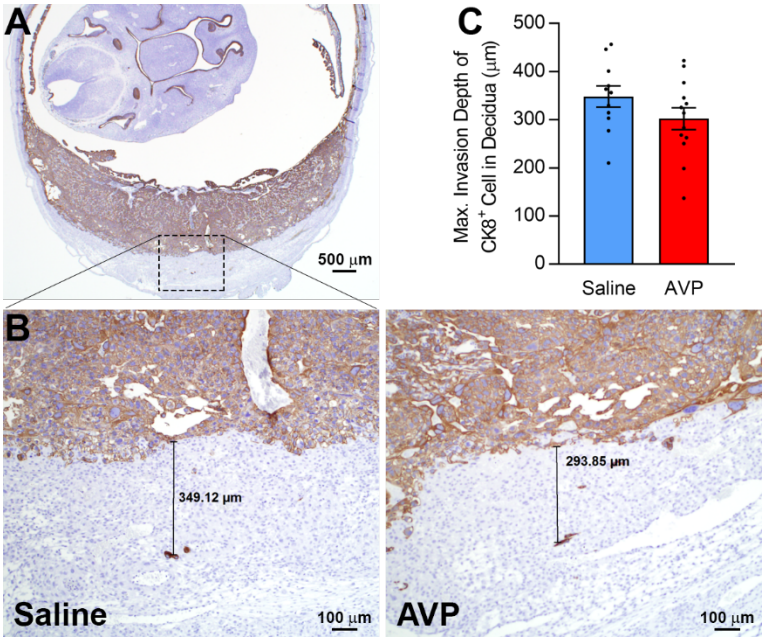

<u>Supplemental Figure 5</u>: *Immunohistochemical staining for cytokeratin-8 (CK8) reveals normal depth of invasion at GD 12.5.* (**A**) Example low-magnification cross-section of feto-placental unit. (**B**) Example high-magnification images of CK8-stained sections, with quantifications of maximal invasion depth illustrated for representative saline- (left) and AVP-treated (right) dams. (**C**) Quantitative data. Individual values plotted represent n=11 saline- and n=13 AVP-treated dams, with multiple stained sections sampled from multiple feto-placental units averaged within each dam before inclusion within the dataset. Data presented as mean ± SEM.

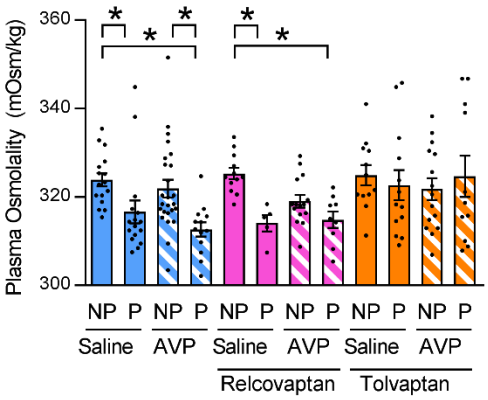

Supplemental Figure 6: *Plasma osmolality.* Plasma osmolality in non-pregnant (NP) and pregnant (P) mice receiving saline or AVP in combination with relcovaptan or tolvaptan. N's: Saline NP=16, Saline P=16, AVP NP=25, AVP P=13, Relcovaptan Saline NP=12, Relcovaptan Saline P=5, Relcovaptan AVP NP=15, Relcovaptan AVP P=9, Tolvaptan Saline NP=12, Tolvaptan Saline P=13, Tolvaptan AVP NP=15, Tolvaptan AVP P=11. Analysis by Tukey's multiple comparisons procedure. Data shown as mean ± SEM. *p<0.05.

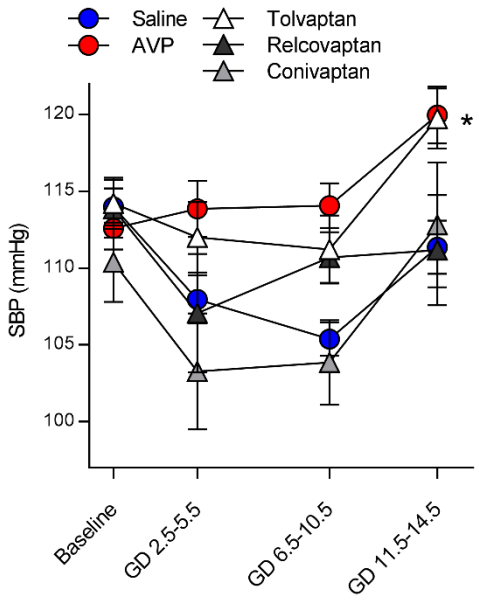

Supplemental Figure 7: *Effect of AVP antagonists on systolic blood pressure (SBP) in pregnant mice without co-infusion of exogenous AVP.* Conivaptan (n=8) and relcovaptan (n=10) and tolvaptan (n=14) effects on SBP throughout pregnancy. Analysis by Tukey's multiple comparisons procedure. Data shown as mean ± SEM. *p<0.05 relative to saline at same GD.

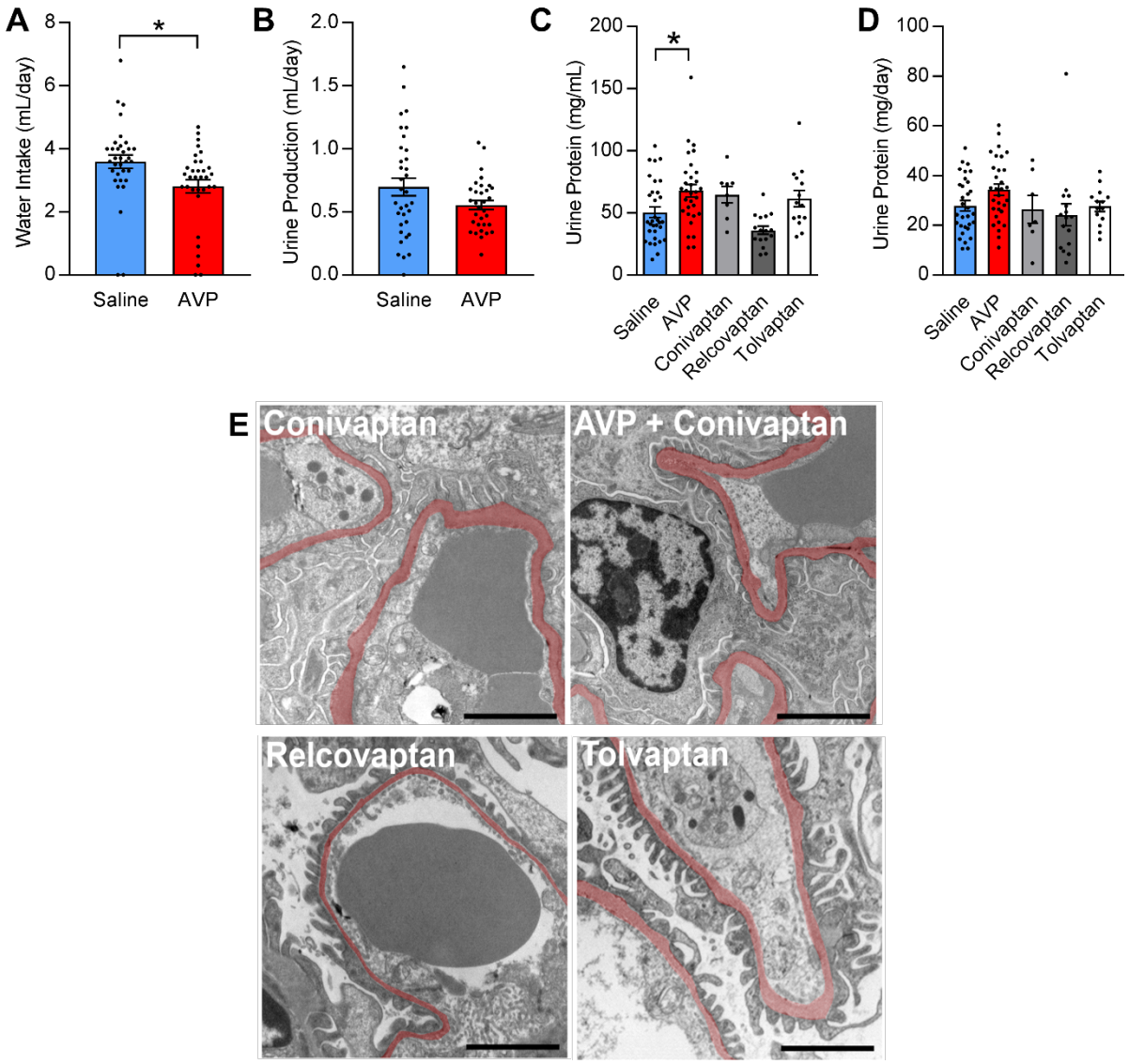

Supplemental Figure 8: *Additional fluid balance and renal phenotypes not reported in main text.* (**A**) Water intake and (**B**) urine production at GD17.5 (Saline n=34, AVP n=32). (**C, D**) AVP antagonist effects on urine protein (Saline n=32, AVP n=30, Conivaptan n=8, Relcovaptan n=16, Tolvaptan n=14). (**E**) Conivaptan, relcovaptan, and tolvaptan effects on the glomerulus (representative images of n=3 for each group). Scale bars = 2 microns. Analyses by Student's t-test (A, B) or Tukey's test for multiple comparisons (C, D). Data shown as mean ± SEM. *p<0.05.

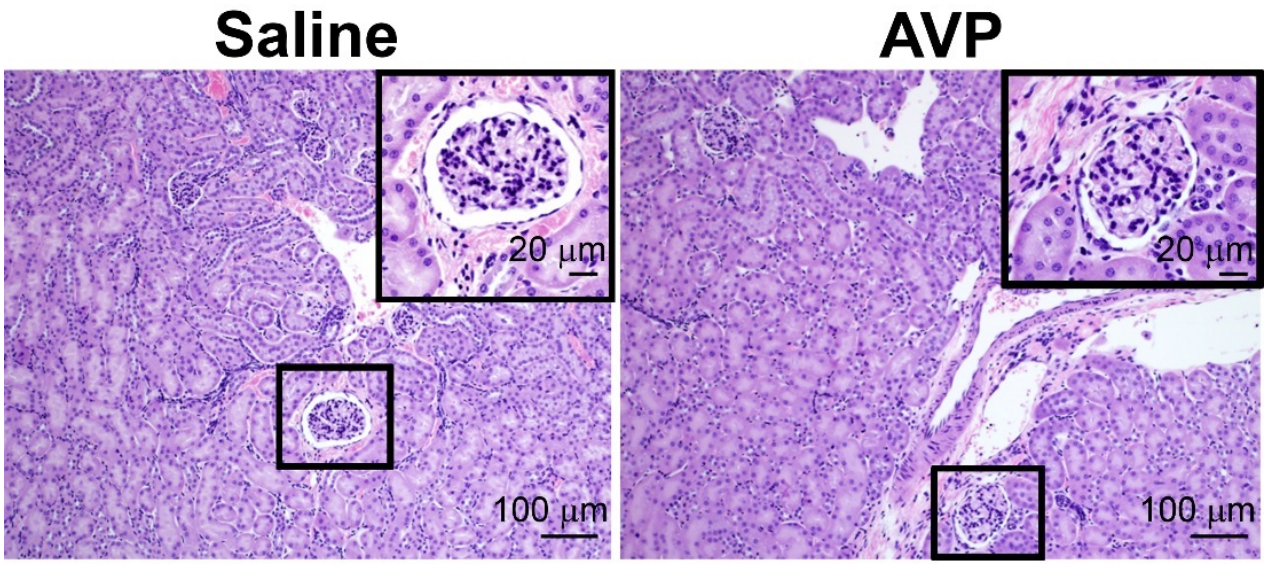

Supplemental Figure 9: *Light microscopic imaging of hematoxylin & eosin-stained kidney sections, illustrating renal tubular and glomerular (inset) morphology of pregnant mice on GD 17.5 following chronic subcutaneous infusion with AVP (24 ng/hr) versus saline.* Images are representative of n=5 mice per group.

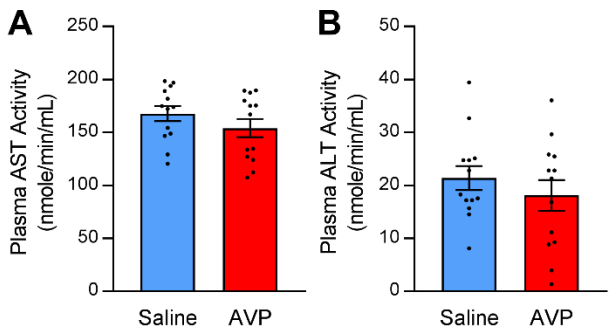

Supplemental Figure 10: *Circulating markers of hepatic dysfunction / damage are unchanged in pregnant mice on GD 17.5 following chronic subcutaneous infusion with AVP (24 ng/hr) versus saline*. (**A**) Plasma activity of aspartate aminotransferase (AST) determined using colorimetric assay from Sigma-Adrich (MAK055). (**B**) Plasma activity of alanine aminotransferase (ALT) determined using colorimetric assay from Sigma-Aldrich (MAK052). Analyses by Student's t-test; n=13 each. Data shown as mean ± SEM.